RSC Chemical Biology

ROYAL SOCIETY OF CHEMISTRY

PAPER

View Article Online
View Journal | View Issue

Cite this: *RSC Chem. Biol.*, 2025, **6**, 1174

Biochemical characterization of *Bifidobacterium bifidum* peptidoglycan D,L-endopeptidase BbMep that generates NOD2 ligands†

Jeric Mun Chung Kwan, [ab] Shiliu Feng, [a] Evan Wei Long Ng [a] and Yuan Qiao *[a]

Received 9th April 2025,
Accepted 30th May 2025

DOI: 10.1039/d5cb00086f

rsc.li/rsc-chembio

Soluble peptidoglycan fragments produced by the gut bacteria are key effectors in microbiota–host crosstalk. Here, we biochemically characterized BbMep, an NlpC/p60 domain-containing peptidoglycan D,L-endopeptidase from *Bifidobacterium bifidum*, which efficiently digests Lys- or Orn-type sacculi. Digestion of human stool-derived muropeptides by BbMep enhances NOD2 activation.

Introduction

The gut microbiota secretes a wide range of small molecules and metabolites, such as short-chain fatty acids, bile acid metabolites, and indole derivatives that profoundly impact host physiology.[1–3] Notably, gut bacteria-derived peptidoglycan fragments (PGNs), abundant in the gut lumen and ubiquitously present in the systemic circulation, are increasingly recognized for their diverse roles in regulating host functions, including altering the host brain activity for proper appetite and body temperature control in female mice,[4] promoting postnatal growth in undernourished infant mice,[5] potentiating checkpoint inhibitor cancer immunotherapy,[6] and regulating gut homeostasis and exerting anti-colitis effects in female mice.[7] Considering the potential of gut bacteria-derived PGNs as novel immunotherapeutics,[8] gaining a deeper understanding of the PGN generation process by the gut microbiota is crucial.

Peptidoglycan is the primary structural component of the cell wall that is conserved across all bacterial species. In general, peptidoglycan is composed of long glycan chains of alternating residues of *N*-acetylglucosamine (GlcNAc) and *N*-acetylmuramic acid (MurNAc) connected *via* the β-1,4-glycosidic bond, with a stem peptide appended to the lactoyl moiety of MurNAc. The stem peptides on adjacent glycan strands can be cross-linked, strengthening the peptidoglycan mesh to withstand the internal turgor pressure in bacteria.[9,10] Given the essential role of peptidoglycan for bacterial survival, each bacteria encodes a suite of enzymes involved in the biosynthesis, assembly, remodelling, and disassembly of the peptidoglycan polymer.[11–15] To accommodate the insertion of new peptidoglycan strands, the existing bacterial peptidoglycan polymer is continuously degraded enzymatically at specific glycosidic or peptide bonds during bacterial growth. This process produces soluble PGNs that are either recycled by the bacteria[16] or released into the surrounding environment. Many of the PGNs released by bacteria are known to function as key signalling molecules in both intra- and inter-kingdom communication in nature.[1,17–19]

The peptidoglycan D,L-endopeptidase is a peptidoglycan remodelling enzyme that features the NlpC/p60 domain (InterPro[20] accession: IPR000064).[21,22] While some NlpC/p60 enzymes are known to cleave other bonds in peptidoglycan,[21,22] a large number of these enzymes specifically cleave the peptide bond between the second and third residue of the stem peptide in peptidoglycan, generating a dipeptide-containing muropeptide (*i.e.* GMDP) and a terminal peptide (*i.e.* TerP) as products (Fig. 1A). Earlier studies have identified and characterized peptidoglycan D,L-endopeptidases in *Lactobacilli*,[23–25] and *Mycobacterium*,[26–28] establishing their importance in bacterial cell morphology and division. Recently, gut bacteria-encoded D,L-endopeptidases have garnered attention due to their biological significance in gut microbiota–host crosstalk.[21] In particular, the GMDP moiety produced by D,L-endopeptidases acts as a potent agonist of the mammalian NOD2 innate immune sensor,[29–31] triggering downstream NF-κB signalling and influencing the proper crosstalk between the gut microbiota and the host. Hang and coworkers have extensively characterized the *Enterococcus* D,L-endopeptidase SagA, showcasing its capability to enhance host immunity and confer tolerance to pathogens.[6,32–35] Moreover, Gao *et al.* reported that both *Firmicutes*-derived

[a] *School of Chemistry, Chemical Engineering and Biotechnology, Nanyang Technological University, 21 Nanyang Link, 637371, Singapore. E-mail: yuan.qiao@ntu.edu.sg*
[b] *Lee Kong Chian School of Medicine, Nanyang Technological University, 11 Mandalay Road, 308232, Singapore*

† Electronic supplementary information (ESI) available. See DOI: https://doi.org/10.1039/d5cb00086f

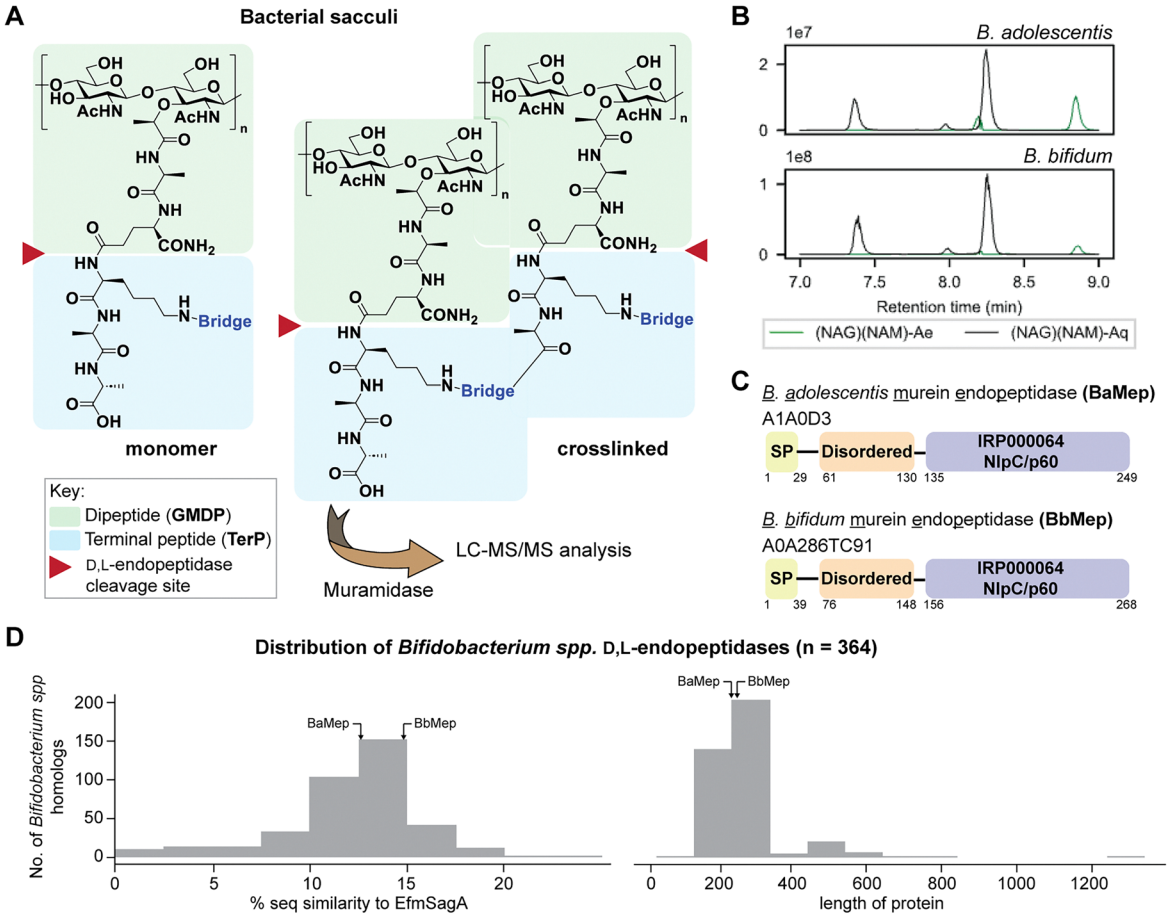

Fig. 1 (A) Peptidoglycan D,L-endopeptidases cleave bacterial sacculi or larger muropeptides into dipeptide (GMDPs) and terminal peptide products (TerPs). GMDPs are liberated only if the sacculus is further treated with a muramidase (*e.g.* lysozyme and mutanolysin). (B) GMDPs have been previously found to be prominent in the peptidoglycan composition of *B. adolescentis* and *B. bifidum* through LC-MS/MS analysis. The two GMDP products shown are (NAG)(NAM)-Ae ($C_{27}H_{44}N_4O_{17}$, $[M + H]^+$ = 697.277) and (NAG)(NAM)-Aq ($C_{27}H_{45}N_5O_{16}$, $[M + H]^+$ = 696.293). (C) Both *Bifidobacterium* species encode a D,L-endopeptidase that contains the NlpC/p60, which are referred to as BaMep and BbMep. The specific domains in BaMep and BbMep are determined by SignalP, MobiDB, and InterPro. SP: signal peptide. (D) Histograms showing the distributions of 364 putative NlpC/p60 endopeptidases in the *Bifidobacterium* genus in terms of sequence similarity (to EfmSagA) (left) and protein lengths (right).

D,L-endopeptidases and *Lactobacillus*-secreted bifunctional hydrolases (LPH) (with D,L-endopeptidase activity), exert anti-colitis effects in mice *via* the generation of NOD2 ligands.[7,36] Given the widespread prevalence of D,L-endopeptidases in the gut microbiome,[36] we set out to explore other uncharacterized gut bacteria-encoded D,L-endopeptidases, which may provide a novel outlook for modulating gut microbiota-derived bioactive PGNs.

In our previous work, we utilized our PGN_MS2 workflow for automated profiling of bacterial peptidoglycan composition in a panel of gut bacteria.[37] Interestingly, we observed that *Bifidobacterium adolescentis* and *Bifidobacterium bifidum* manifest elevated levels of D,L-endopeptidase products (GMDP) in their sacculi (Fig. 1B), implying both *Bifidobacterium* species encode highly active peptidoglycan D,L-endopeptidases.[37] In this study, we identified the peptidoglycan D,L-endopeptidase, BbMep, in *B. bifidum*, and biochemically reconstituted its activity. In addition, we show that it is capable of effectively generating bioactive NOD2 ligands.

Results and discussion

Identification of *Bifidobacterium* NlpC/p60 D,L-endopeptidase by sequence homology

To identify the putative *Bifidobacterium* D,L-endopeptidases, we searched the proteomes of *B. adolescentis* ATCC 15703 and *B. bifidum* ATCC 15696 for proteins containing the known endopeptidase catalytic domains (*i.e.*, NlpC/p60 or peptidase M14) using UniProt.[38] While no homologs of *E. coli* MpaA[39] containing the peptidase M14 domain (IPR000834) were identified in *Bifidobacterium*, we found that both *Bifidobacterium* species possess proteins with NlpC/p60 catalytic domains, A1A0D3 and A0A286TC91, which we will refer to as BaMep and BbMep, where Mep represents **m**urein **endop**eptidase. Both proteins encode a predicted N-terminus signal peptide, a disordered region, and a single NlpC/p60 domain (Fig. 1C). Expanding our search to the *Bifidobacterium* genus, we found 364 NlpC/p60 endopeptidase proteins, which were classified into three distinct clusters based on sequence similarity (Fig. S1, ESI†).

Interestingly, *Bifidobacterium* endopeptidases displayed weak similarity to EfmSagA, with identities below 20%, and the majority have protein lengths ranging from 150 to 250 amino acids (Fig. 1D). Most of them lack the predicted coiled-coil domain present in EfmSagA.[33,34]

Evaluation of *Bifidobacterium* endopeptidase activity with bacterial sacculi

We cloned, overexpressed, and purified the full-length constructs of BaMep (30–249 aa) and BbMep (40–268 aa) that lack the signal peptide, as well as the truncated versions, Ba_SD (135–249 aa) and Bb_SD (156–268 aa), that contain the NlpC/p60 domain solely. The yields of the four recombinant *Bifidobacterium* endopeptidases were ~10 mg L^{-1} of *E. coli* culture, while the solubility and folding of each were evaluated by size-exclusion chromatography (SEC) (Fig. S2 and S3, ESI†). As a positive control, EfmSagA was purified following the protocol from Hang and coworkers.[33]

To evaluate peptidoglycan endopeptidase activity, we treated recombinant BaMep and BbMep with native sacculi isolated from *B. adolescentis* and *B. bifidum*, respectively, for overnight incubation at 37 °C, followed by heat inactivation; lysozymes were then added to the crude reaction mixture to liberate soluble PGNs for LC-MS analysis (Fig. 2A). In LC-MS analysis, we compared the total peak areas of GMDP and TerP products as a measure of D,L-endopeptidase activity. To control for the amount of sacculi suspension used, we utilized the naturally occurring moiety (NAG)(NAM)-A as an internal standard, since its concentration is unaffected by D,L-endopeptidase activity. Although we observed a slight reduction in crosslinked and monomeric tetrapeptide products with BaMep (Table S1, ESI†), we did not observe increased amounts of GMDP/TerP products (Fig. 2B), suggesting a lack of endopeptidase activity. However, we could not rule out the possibility of other enzymatic activities. On the other hand, we found that BbMep exhibited robust D,L-endopeptidase activity, producing elevated amounts of GMDP and TerP from isolated sacculi (Fig. 2B, Fig. S4 and Table S2, ESI†).

To rule out that native *Bifidobacterium* peptidoglycan serves as a poor substrate due to intrinsic D,L-endopeptidase modification, we next investigated the activities of BbMep and BaMep using a panel of bacterial sacculi isolated from *E. faecalis*, *E. faecium*, *S. aureus*, and *E. coli* as substrates. EfmSagA was included as a positive control. Unfortunately, BaMep did not produce GMDP/TerP products *in vitro* (Fig. 2C and Tables S3–S6, ESI†), indicating its lack of D,L-endopeptidase activity under the current experimental conditions. Additional protein partners or proteolysis may be required for BaMep activation, which was not explored in this study.

On the other hand, BbMep exhibits selective activity on Lys-type sacculi (*E. faecalis*, *E. faecium*, *S. aureus*) but did not cleave mDAP-type sacculi (*E. coli*), similar to EfmSagA (Fig. 2C, Fig. S5–S7, Tables S3–S6, ESI†). Notably, the endopeptidase activity of BbMep on *E. faecium* sacculi was comparable to that of EfmSagA, whereas its activity on *S. aureus* and *E. faecalis* sacculi was significantly lower than on its native sacculi and *E. faecium* sacculi. In addition, we showed that the domain-only construct Bb_SD retains similar activity to the full-length BbMep (Fig. 2C), confirming that the NlpC/p60 domain was responsible for its enzymatic activity. Based on the *in vitro* observations, we proposed that the amino acid composition of the peptide bridge in the bacterial sacculi substrate might be critical for the robust activity of BbMep. In particular, peptide bridges containing polar amino acid residues, such as Ser-Asp or Asp/Asn (as found in the peptidoglycan of *E. faecium* and *B. bifidum*),[37] are preferred over those composed solely of non-polar residues like Gly_5 and Ala_2 (as in *S. aureus* and *E. faecalis*). As we previously reported, *B. bifidum* natively contains Orn primarily (with Lys as a minor component) as the third amino acid in the stem peptide.[37] Here, our results indicate that substituting Orn with Lys does not interfere with BbMep activity, whereas mDAP-containing peptidoglycan was not a suitable substrate. Together, these findings suggest that BbMep can cleave sacculi from Gram-positive bacterial species, supporting its potential role as a secreted protein with implications for modulating gut-derived bacteria PGNs.

Previous studies have reported that NlpC/p60-containing peptidoglycan D,L-endopeptidases exhibit substrate preference on cross-linked peptidoglycan.[24,25,34] Hence, we closely examined the identities of the TerP products released by BbMep from sacculi isolated from Gram-positive bacteria. Interestingly, both terminal peptide monomers and larger, crosslinked terminal peptides were identified (Fig. S4–S7, ESI†), potentially originating from non-crosslinked and crosslinked peptidoglycan substrates (Fig. 1A). Specifically, we identified 4, 9, 14 and 9 different types of TerPs from BbMep-digested sacculi of *B. bifidum*, *E. faecium*, *E. faecalis*, and *S. aureus*, respectively (Fig. S4–S7, ESI†). To directly explore whether BbMep uses monomeric non-crosslinked muropeptides as substrates, we tested its activity with a panel of six synthetic or isolated muropeptide standards, each bearing a stem peptide of three to five amino acids in length (Fig. S8A, ESI†). Unfortunately, no cleavage product was observed with mono-saccharide Lys-type muropeptides (tetrapeptide 1 & pentapeptide 3), di-saccharide Lys-type tripeptide 2, or di-saccharide mDAP-type tetrapeptides (4 & 5). Additionally, BbMep did not cleave the di-saccharide pentapeptide with a pentaglycine bridge (6), which we had isolated from the large-scale digestion of *S. aureus* sacculi.[40] Our results suggest that BbMep cannot utilize non-crosslinked monomeric muropeptides as substrates (Fig. S8B, ESI†).

Sequence alignment reveals key residues in BbMep for activity

Intrigued by the disparity in activity between BbMep and BaMep, we sought to explore their underlying molecular differences by aligning their protein sequences with those of other NlpC/p60 domain D,L-endopeptidases of known activity (Fig. 3A). Strikingly, the phylogenetic tree analysis revealed that both BbMep and BaMep were only distantly related to other NlpC/p60 proteins, which share a closer resemblance to the previously characterized EfmSagA (Fig. 3B). Nevertheless, both BaMep and BbMep contain the catalytic Cys and His dyad (BaMep: C166 & H212 and BbMep: C186 & H233) that is well-conserved across all members of the NlpC/p60 family (Fig. 3A).[35] Moreover, Kim *et. al*

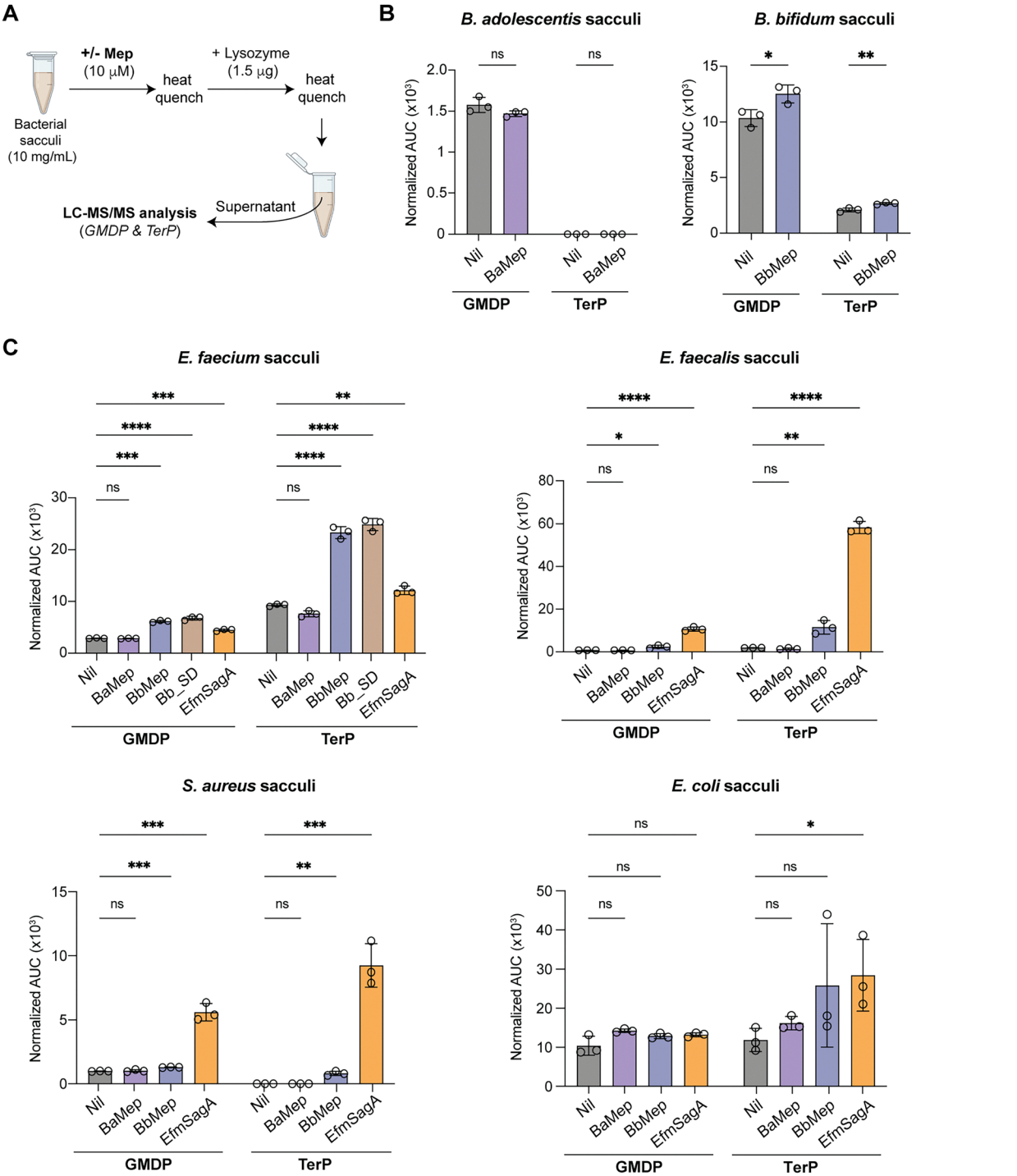

Fig. 2 (A) Schematic showing biochemical assay of endopeptidases. (B) and (C) LC-MS/MS analysis of quantification of GMDP and TerP products released by endopeptidase digestion of various bacterial sacculi. Bb_SD contains the NlpC/p60 domain only (residues 156–268). The muropeptide (NAG)(NAM)-A was used as an internal standard for peak area normalization. Error bars represent the standard deviations of the mean of three independent replicates. *p*-Values were calculated with a two-tailed student's *t*-test ($\alpha = 0.05$, $n = 3$), comparing each enzyme with the negative control (Nil). *p*-Values were adjusted for multiple comparisons with the Bonferroni method. *$p < 0.05$; **$p < 0.01$; ***$p < 0.001$; ****$p < 0.0001$; ns: not significant.

previously identified two Trp residues in EfmSagA, W429 and W458, as substrate-binding residues essential for its endopeptidase activity (indicated by triangles, Fig. 3A),[34] herein referred to as Trp1 and Trp2, respectively. Our sequence alignment indicates that while Trp1 is highly conserved in D,L-endopeptidases from several bacteria species, including *Enterococcus*, *Lactobacillus*, and *Mycobacterium*, Trp2 is strictly conserved only in *Enterococcus*, suggesting that Trp1 may be more critical for function than the

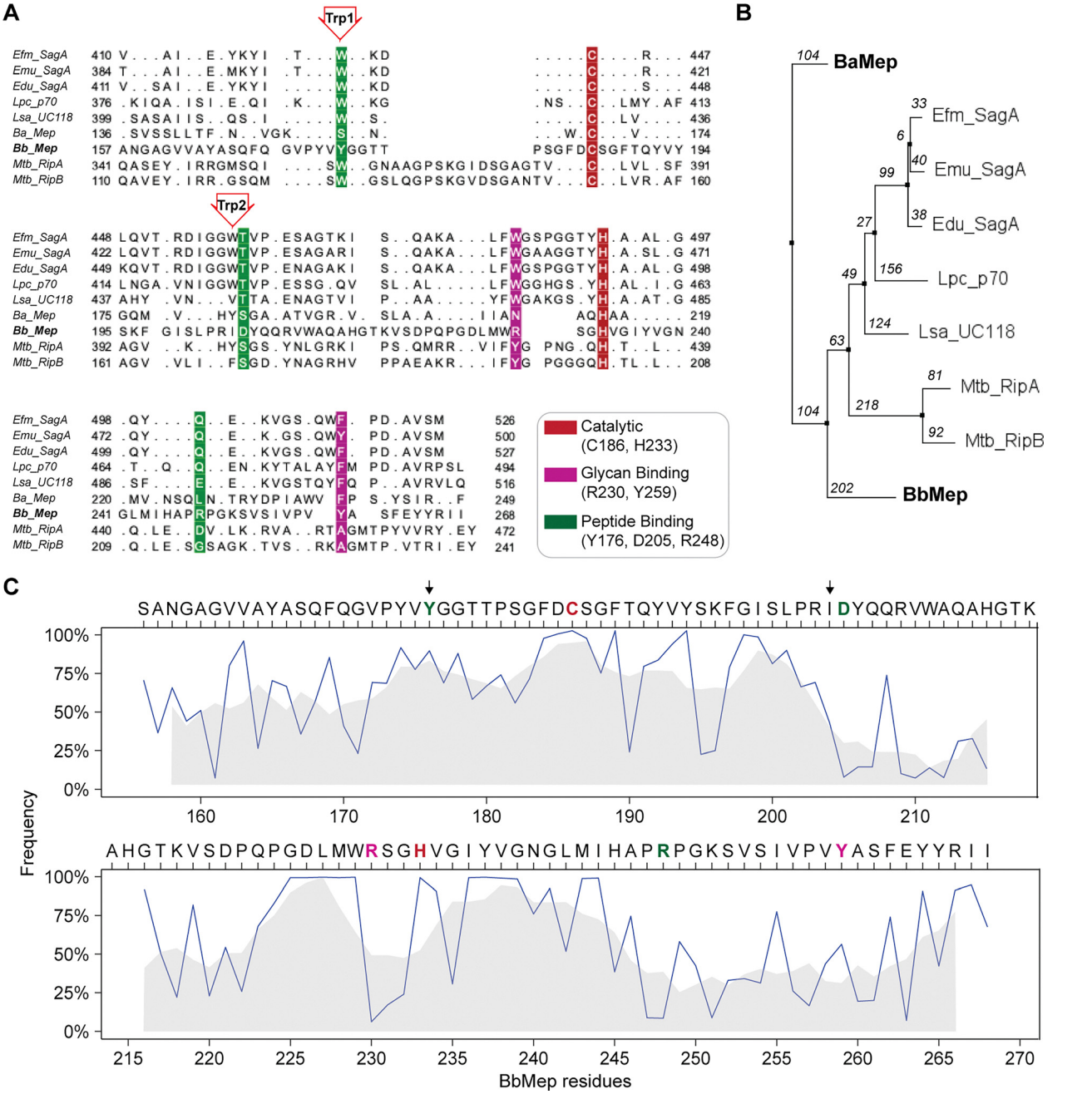

Fig. 3 (A) and (B) Multiple sequence alignment and phylogenetic tree of BaMep and BbMep with other peptidoglycan D,L-endopeptidases with known activity. Numbers on the phylogenetic tree indicate the computed BLOSUM62 distance. *Enteroccocus*: Efm = *E. faecium,* Emu = *E. mundtii,* and Edu = *E. durans*; *Lactobacillus*: Lpc = *L. paracasei* and Lsa = *L. salivarius*; *Bifidobacterium*: Ba = *B. adolescentis* and Bb = *B. bifidum*; *Mycobacterium*: Mtb = *M. tuberculosis.* (C) Percentage of BbMep residue conservation (full or partial) across 364 putative *Bifidobacterium* endopeptidases. The black arrows indicate residues aligned to W429 (Trp1) and W458 (Trp2) from EfmSagA. The catalytic residues C186 and H233 in BbMep are bolded in red. The predicted glycan- and peptide-binding residues in BbMep (from the docking analysis in next section) are indicated in magenta and green, respectively. The grey area indicates the running average for five residues.

second. Interestingly, neither *Bifidobacterium* homologs strictly conserve Trp1 and Trp2. Instead, BbMep has Y176/I204 and BaMep has S156/Y184 at the corresponding positions (Fig. 3A). Given the robust cleavage activity of BbMep and the lack of activity in BaMep, our findings support the idea that Trp1 is likely more critical for enzymatic function, which is partially conserved in BbMep as Tyr, an alternative hydrophobic, aromatic amino acid (*i.e.*, Y176). Indeed, among the 364 putative *Bifidobacterium* NlpC/p60 endopeptidases, Trp1 is partially or strictly conserved to a larger extent compared to Trp2 (87% *vs.* 40%) (Fig. 3C). Moreover, we also examined the conservation of BbMep residues across *Bifidobacterium* endopeptidases (Fig. 3C). Interestingly, four regions

appear to be largely conserved: residues 174–189, residues 197–201, residues 222–239 and 235–245. Of note, both Y176 (Trp1 in EfmSagA) and the catalytic residue C186 are located in the first conserved region (Fig. 3C).

BbMep exhibits strong binding to bacterial sacculi

In our aforementioned *in vitro* cleavage assay, we treated BbMep and EfmSagA with bacterial sacculi before the addition of lysozyme, demonstrating that both enzymes can utilize isolated sacculi as substrates. This observation contrasts with previous reports suggesting that EfmSagA acts only on pre-digested sacculi (treated with lysozyme or mutanolysin).[33,34] Interestingly, we also found that BbMep exhibits greater endopeptidase activity on *E. faecium* sacculi compared to the cognate EfmSagA (Fig. 2C). We propose that the difference in activity could arise from their distinct binding affinities for the sacculi substrates. To study this, we performed sedimentation assays of respective proteins with *E. faecium* sacculi (Fig. 4A and Fig. S9A, B, ESI†). Indeed, BbMep and its domain-only construct BbSD exhibited strong binding to sacculi, with all proteins bound to the insoluble sacculi fraction and minimal recovery in the supernatant. In contrast, EfmSagA showed weak sacculi binding, with most of the protein remaining in the supernatant.

Determination of sacculi-binding residues in BbMep

To identify the residues in BbMep responsible for sacculi binding, we performed *in silico* molecular docking of a mock PGN ligand (GM-AqKAA) into the active site of the predicted BbMep structure generated by AlphaFold2 (AF2) (Fig. 4B).[41] As it was known that removal of low-confidence (*i.e.* pLDDT score <70) residues in AF2 structures can yield greater docking accuracy,[42] we omitted residues with pLDDT scores <70 from the AF2 predicted structure, yielding AF2-BbMep (158–268). We note that the omitted region corresponded to the N-terminus that contains the predicted signal peptide and an unstructured region (Fig. 1C). The remaining region corresponds to the NlpC/p60 domain, with most residues having pLDDT scores in the range of 90–100, indicating a high level of confidence in the accuracy of their positions.[41] Indeed, the predicted structure of BbMep contains the three N-terminal α helixes and subsequent five-stranded beta sheet common in NlpC/p60 peptidoglycan endopeptidases.[21,22]

From the multiple docking poses (3 runs × 10 poses) generated by AutoDock Vina,[43] we selected the most promising poses based on two criteria: (1) the calculated binding affinity (kcal mol^{-1}) and (2) the ''catalytic distance'', the distance between the catalytic residue (BbMep_C186) and the specific peptide bond in the PGN ligand that undergoes cleavage (Fig. S10A, B, ESI†). We note that in the reported co-crystal structure of YkFC, a *Bacillus cereus* NlpC/p60 D,L-endopeptidase, with dipeptide L-Ala-γ-D-Glu (PDB 3H4-1), the catalytic distance from the Cα of the catalytic Cys (OCS-238) to the carbonyl carbon of the peptide substrate was 7.3 Å (Fig. S10A, ESI†),[44] providing a useful reference for our docking study. Therefore, we focused on the docked poses of AF2-BbMep (158–268) with binding affinity <-6 kcal mol^{-1} and catalytic distance <7.5 Å for further analysis with LigPlot+[45] (Fig. S10C and Table S7, ESI†). 5 of the 30 poses fit these criteria. Based on the rationale that the sacculi-binding residues in BbMep likely differ from those in EfmSagA, which is not a potent sacculi binder (Fig. 4A), we proposed that residues Y259 and R230 may be involved in binding to the glycan moiety of sacculi, whereas residues D205, Y176, and R248 may engage in binding to the peptide moiety (Fig. 4B, C and Fig. S10D, ESI†). Although S231 is dissimilar to the corresponding residue in EfmSagA (T), we did not select it for further analysis as a plurality of the other characterized endopeptidases also contain Ser at this position (44%, Fig. 3A). Importantly, these residues form multiple H-bonds in the docking models of BbMep (Fig. 4C and Fig. S10D, ESI†). Interestingly, the peptide-binding residue Y176 corresponds to Trp1. As previously noted, this residue in EfmSagA was identified by Kim *et al.* as a key factor for muropeptide recognition and interaction,[34] thereby validating our docking-assisted approach for identifying potential substrate-binding residues in BbMep. Interestingly, except for Y176, which we previously showed to be well conserved in *Bifidobacterium*, the other four are either less conserved (Y259:56%) or not conserved (R230, D205, and R248: $<10\%$) amongst *Bifidobacterium* endopeptidases (Fig. 3C). This possibly suggests that BbMep's sacculi binding properties might be unique amongst *Bifidobacterium* endopeptidases.

Characterization of BbMep mutants that are deficient in sacculi binding

To test our hypothesis about the predicted BbMep residues involved in sacculi binding, we generated three mutant variants: BbMep Mut1 (glycan-binding deficient mutant; Y259A and R230A mutations), Mut2 (peptide-binding deficient mutant; D205A, Y176A, and R248A), and Mut3 (catalytic residue-absent mutant; C186A) (Fig. 4D). The mutant proteins were expressed and purified (Fig. S3, ESI†). In the *in vitro* binding assay, we incubated the respective BbMep variants (10 μM) with sacculi at varying concentrations ranging from 0 to 20 mg mL^{-1} (Fig. 4E and Fig. S9D, ESI†). Indeed, both Mut1 and Mut2 exhibited reduced binding to sacculi substrates, with a more pronounced effect observed for Mut1, which is presumably deficient in binding to the glycan moiety of sacculi. On the other hand, Mut3 shows sacculi binding comparable to that of the wild-type protein, consistent with the idea that the catalytic residue C186 is not directly involved in substrate binding.

Next, we evaluated the enzymatic activity of BbMep mutant variants with *E. faecium* sacculus. As expected, BbMep Mut3, which lacks the catalytic residue, is completely inactive (Fig. 4F and Table S8, ESI†). In addition, both Mut1 and Mut2 also exhibited weaker endopeptidase activity, as evidenced by the lower abundance of the cleavage products GMDP and TerP (Fig. 4F). Notably, Mut2, which has reduced binding to the stem peptide, exhibited lower activity in comparison with Mut1 (10% *vs.* 50% activity of wild type BbMep). We reasoned that this is likely due to the involvement of the peptide bond within the stem peptide at the endopeptidase cleavage site.

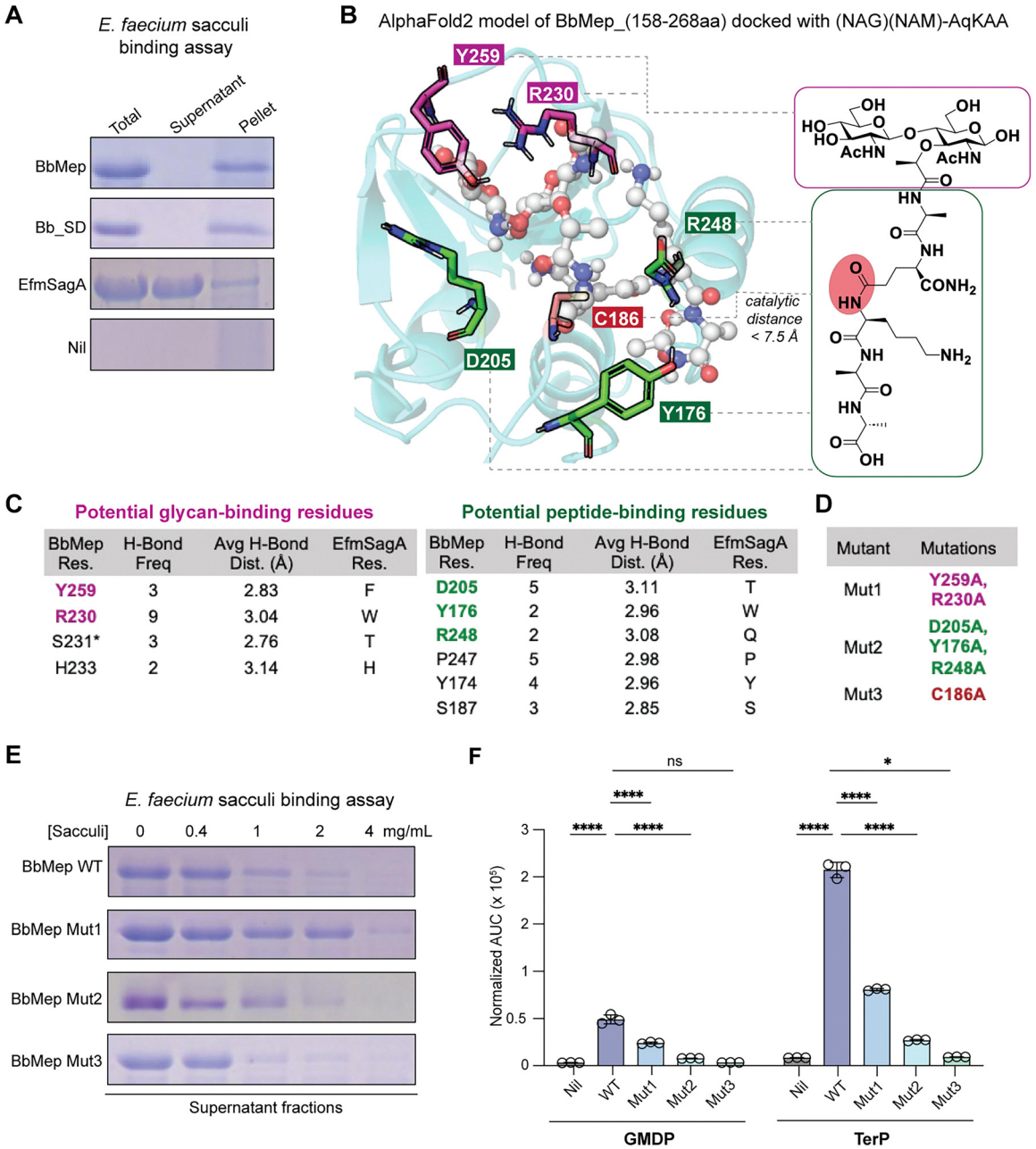

Fig. 4 (A) Sacculi binding assay revealed that BbMep and its NlpC/p60 domain-only construct, BbMep_SD (10 μM) bind to *E. faecium* sacculi (20 mg mL^{-1}), whereas EfmSagA (10 μM) does not. (B) and (C) Prediction of potential PGN-interacting residues in BbMep based on *in silico* molecular docking. The AlphaFold predicted BbMep structure was docked with (NAG)(NAM)-AqKAA using AutoDock Vina. The best docking poses from 3 runs × 10 poses were selected for further analysis (see Fig. S10, ESI†). We selected the docked poses with a binding affinity < -6 kcal mol^{-1} and a catalytic distance < 7.5 Å between C186 and the peptide bond undergoing cleavage. The BbMep residues involved in glycan- (magenta) or peptide-binding (green) meet two criteria: (1) they form one or more hydrogen bonds, and (2) they differ from Efm residues. (D) Construction of BbMep_Mut1, Mut2, and Mut3 to experimentally validate the proposed PGN-interacting residues. (E) and (F) Both Mut1 and Mut2 exhibit slightly reduced binding to bacterial sacculi (E) and significantly reduced endopeptidase activity in LC-MS analysis (E). The muropeptide (NAG)(NAM)-A was used as an internal standard for peak area normalization in LC-MS. Error bars represent the standard deviations of the mean of three independent replicates. *p*-Values were calculated with a two-tailed student's *t*-test ($\alpha = 0.05$, $n = 3$), comparing each group with the wild-type BbMep. *p*-Values were adjusted for multiple comparisons with the Bonferroni method. $*p < 0.05$; $****p < 0.0001$; ns: not significant.

BbMep generates NOD2 ligands in the host gut microbiota

Having established the biochemical activity of BbMep with isolated Lys/Orn-type sacculi as substrates, we next investigated whether BbMep could degrade gut microbiota-derived peptidoglycan to yield bioactive PGNs, considering that *B. bifidum* is a resident bacterium in the human gut.[46] To do so, we extracted soluble muropeptides from 12 human stool samples by treating them with lysozyme. The soluble muropeptides were then subjected to

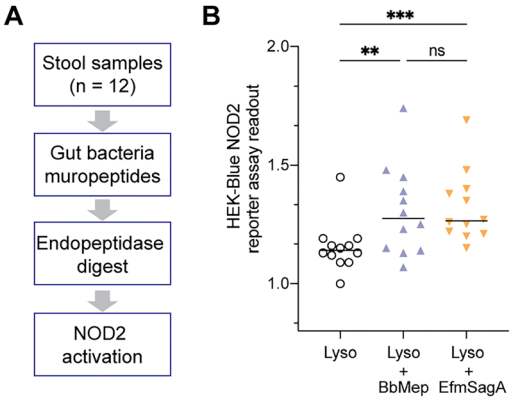

Fig. 5 BbMep, similar to EfmSagA, generates active NOD2 ligands in human stool samples. (A) Protocol of workflow: soluble muropeptides were first extracted from human stool by lysozyme and then treated with BbMep or EfmSagA, followed by analysis using HEK-Blue NOD2 reporter assay. (B) A significant increase in NOD2 induction was observed in both BbMep- and Efm-treated samples compared to non-endopeptidase control. p-Values were calculated with a paired t-test ($\alpha = 0.05$, $n = 12$). $^{**}p < 0.01$; $^{****}p < 0.0001$; ns: not significant.

endopeptidase digestion with BbMep (10 μM) or EfmSagA (10 μM) or left untreated. The NOD2-activating effects were evaluated using HEK-blue hNOD2 reporter assays (Fig. 5A). Compared to the non-endopeptidase control, treatment with either BbMep or EfmSagA resulted in a significant increase in NOD2 activity, indicating that BbMep generates bioactive NOD2 agonists (Fig. 5B). Importantly, BbMep shows robust activity that is comparable to EfmSagA, and addition of either enzyme results in a modest 10% increase in the amount of NOD2 agonists compared to the negative control. Considering the biological significance of NOD2 agonists generated by EfmSagA in enhancing host immunity and potentiating cancer immunotherapy[6,34,47] and the protective effects of *Lactobacillus* D,L-endopeptidase-generated PGNs against colitis and inflammation-associated colorectal cancer,[7,36] our findings that BbMep exhibits similar cleavage activity to gut bacteria-derived PGNs underscore its untapped therapeutic potential to benefit host health.

Conclusions

In summary, we characterized BbMep, the putative secreted D,L-endopeptidase from *B. bifidum*, which acts on the sacculi of Gram-positive bacteria. We identified key residues of BbMep that are essential for both sacculi binding and enzymatic activity. Lastly, BbMep digestion of stool-derived muropeptides enhances NOD2 activation, highlighting its potential to modulate bioactive PGNs for host health.

Author contributions

J. M. C. K. and Y. Q. designed the research; J. M. C. K. and E. W. L. N. performed molecular cloning, protein expression, and purification; J. M. C. K. performed sequence alignment, isolation of sacculi; LC-MS/MS-based biochemical characterization, peptidoglycan binding assays, and *in silico* docking analysis; E. W. L. N. optimized the protocol for isolation of muropeptides from stool; J. M. C. K. and E. W. L. N. isolated muropeptides from stool samples; S. F. performed the *in vitro* assays with HEK-Blue reporter cells; J. M. C. K., S. F. and Y. Q. analysed the data; Y. Q. supervised the work; J. M. C. K. and Y. Q. wrote the paper with inputs from all authors.

Data availability

The data supporting this article have been included as part of the ESI.† The sequences for BaMep and BbMep can be found on UniProt (accession IDs: A1A0D3 (**https://www.uniprot.org/uniprotkb/A1A0D3/entry**) and A0A286TC91 (**https://www.uniprot.org/uniprotkb/A0A286TC91/entry**) respectively). The AlphaFold2 (**alphafold.ebi.ac.uk/entry/A0A286TC91**) structure for BbMep can be found in the AlphaFold Protein Structure Database.

Conflicts of interest

There are no conflicts to declare.

Acknowledgements

We acknowledge members of the Qiao lab for critical reading of the manuscript. J. M. C. K.'s PhD candidature is supported by the Nanyang Presidential Graduate Scholarship. S. F.'s PhD candidature is supported by the NTU Research Scholarship. This work was supported by the National Research Foundation (NRF) Singapore, NRF-NRFF12-2020-0006, NTU-Start-up grant, and MOE-T2EP30223-0002, MOET2EP10124-0001, to Y. Q.

Notes and references

1 C. Li, Y. Liang and Y. Qiao, *Front. Microbiol.*, 2022, **13**, 863407.
2 F. Sommer and F. Bäckhed, *Nat. Rev. Microbiol.*, 2013, **11**, 227–238.
3 A. Agus, K. Clément and H. Sokol, *Gut*, 2021, **70**, 1174–1182.
4 I. Gabanyi, G. Lepousez, R. Wheeler, A. Vieites-Prado, A. Nissant, S. Wagner, C. Moigneu, S. Dulauroy, S. Hicham, B. Polomack, F. Verny, P. Rosenstiel, N. Renier, I. G. Boneca, G. Eberl and P.-M. Lledo, *Science*, 2022, **376**, eabj3986.
5 M. Schwarzer, U. K. Gautam, K. Makki, A. Lambert, T. Brabec, A. Joly, D. Šrůtková, P. Poinsot, T. Novotná, S. Geoffroy, P. Courtin, P. P. Hermanová, R. C. Matos, J. J. M. Landry, C. Gérard, A.-L. Bulteau, T. Hudcovic, H. Kozáková, D. Filipp, M.-P. Chapot-Chartier, M. Šinkora, N. Peretti, I. G. Boneca, M. Chamaillard, H. Vidal, F. De Vadder and F. Leulier, *Science*, 2023, **379**, 826–833.
6 M. E. Griffin, J. Espinosa, J. L. Becker, J. D. Luo, T. S. Carroll, J. K. Jha, G. R. Fanger and H. C. Hang, *Science*, 2021, **373**, 1040–1046.
7 J. Gao, L. Wang, J. Jiang, Q. Xu, N. Zeng, B. Lu, P. Yuan, K. Sun, H. Zhou and X. He, *Nat. Commun.*, 2023, **14**, 3338.

8 M. E. Griffin, C. W. Hespen, Y.-C. Wang and H. C. Hang, *Clin. Transl. Immunol.*, 2019, **8**, e1095.
9 T. J. Silhavy, D. Kahne and S. Walker, *Cold Spring Harbor Perspect. Biol.*, 2010, **2**, a000414.
10 R. D. Turner, W. Vollmer and S. J. Foster, *Mol. Microbiol.*, 2014, **91**, 862–874.
11 J. M. C. Kwan and Y. Qiao, *ChemBioChem*, 2023, **24**, e202200693.
12 S. Kumar, A. Mollo, D. Kahne and N. Ruiz, *Chem. Rev.*, 2022, **122**, 8884–8910.
13 H. Zhao, V. Patel, J. D. Helmann and T. Dörr, *Mol. Microbiol.*, 2017, **106**, 847–860.
14 A. J. F. Egan, J. Errington and W. Vollmer, *Nat. Rev. Microbiol.*, 2020, **18**, 446–460.
15 A. P. Brogan and D. Z. Rudner, *Curr. Opin. Microbiol.*, 2023, **72**, 102279.
16 C. Mayer, R. M. Kluj, M. Mühleck, A. Walter, S. Unsleber, I. Hottmann and M. Borisova, *Int. J. Med. Microbiol.*, 2019, **309**, 151326.
17 O. Irazoki, S. B. Hernandez and F. Cava, *Front. Microbiol.*, 2019, **10**, 500.
18 J. Dworkin, *Annu. Rev. Microbiol.*, 2014, **68**, 137–154.
19 P. A. D. Bastos, R. Wheeler and I. G. Boneca, *FEMS Microbiol. Rev.*, 2021, **45**, 1–25.
20 M. Blum, H. Y. Chang, S. Chuguransky, T. Grego, S. Kandasaamy, A. Mitchell, G. Nuka, T. Paysan-Lafosse, M. Qureshi, S. Raj, L. Richardson, G. A. Salazar, L. Williams, P. Bork, A. Bridge, J. Gough, D. H. Haft, I. Letunic, A. Marchler-Bauer, H. Mi, D. A. Natale, M. Necci, C. A. Orengo, A. P. Pandurangan, C. Rivoire, C. J. A. Sigrist, I. Sillitoe, N. Thanki, P. D. Thomas, S. C. E. Tosatto, C. H. Wu, A. Bateman and R. D. Finn, *Nucleic Acids Res.*, 2021, **49**, D344–D354.
21 M. E. Griffin, S. Klupt, J. Espinosa and H. C. Hang, *Cell Chem. Biol.*, 2023, **30**, 436–456.
22 V. Anantharaman and L. Aravind, *Genome Biol.*, 2003, **4**, R11.
23 T. Rolain, E. Bernard, P. Courtin, P. A. Bron, M. Kleerebezem, M.-P. Chapot-Chartier and P. Hols, *Microb. Cell Fact.*, 2012, **11**, 137.
24 K. Regulski, P. Courtin, M. Meyrand, I. J. J. Claes, S. Lebeer, J. Vanderleyden, P. Hols, A. Guillot and M.-P. Chapot-Chartier, *PLoS One*, 2012, **7**, e32301.
25 I. J. J. Claes, G. Schoofs, K. Regulski, P. Courtin, M.-P. Chapot-Chartier, T. Rolain, P. Hols, I. von Ossowski, J. Reunanen, W. M. de Vos, A. Palva, J. Vanderleyden, S. C. J. D. Keersmaecker and S. Lebeer, *PLoS One*, 2012, **7**, e31588.
26 D. J. Martinelli and M. S. Pavelka, *J. Bacteriol.*, 2016, **198**, 1464–1475.
27 D. Böth, G. Schneider and R. Schnell, *J. Mol. Biol.*, 2011, **413**, 247–260.
28 E. M. Steiner, J. Lyngsø, J. E. Guy, G. Bourenkov, Y. Lindqvist, T. R. Schneider, J. S. Pedersen, G. Schneider and R. Schnell, *Proteins: Struct., Funct., Bioinf.*, 2018, **86**, 912–923.
29 S. E. Girardin, I. G. Boneca, J. Viala, M. Chamaillard, A. Labigne, G. Thomas, D. J. Philpott and P. J. Sansonetti, *J. Biol. Chem.*, 2003, **278**, 8869–8872.
30 S. E. Girardin, L. H. Travassos, M. Hervé, D. Blanot, I. G. Boneca, D. J. Philpott, P. J. Sansonetti and D. Mengin-Lecreulx, *J. Biol. Chem.*, 2003, **278**, 41702–41708.
31 N. Inohara, Y. Ogura, A. Fontalba, O. Gutierrez, F. Pons, J. Crespo, K. Fukase, S. Inamura, S. Kusumoto, M. Hashimoto, S. J. Foster, A. P. Moran, J. L. Fernandez-Luna and G. Nuñez, *J. Biol. Chem.*, 2003, **278**, 5509–5512.
32 V. A. Pedicord, A. A. K. Lockhart, K. J. Rangan, J. W. Craig, J. Loschko, A. Rogoz, H. C. Hang and D. Mucida, *Sci. Immunol.*, 2016, **1**, eaai7732.
33 K. J. Rangan, V. A. Pedicord, Y.-C. Wang, B. Kim, Y. Lu, S. Shaham, D. Mucida and H. C. Hang, *Science*, 2016, **353**, 1434–1437.
34 B. Kim, Y.-C. Wang, C. W. Hespen, J. Espinosa, J. Salje, K. J. Rangan, D. A. Oren, J. Y. Kang, V. A. Pedicord and H. C. Hang, *eLife*, 2019, **8**, e45343.
35 J. Espinosa, T.-Y. Lin, Y. Estrella, B. Kim, H. Molina and H. C. Hang, *Biochemistry*, 2020, **59**, 4470–4480.
36 J. Gao, X. Zhao, S. Hu, Z. Huang, M. Hu, S. Jin, B. Lu, K. Sun, Z. Wang, J. Fu, R. K. Weersma, X. He and H. Zhou, *Cell Host Microbe*, 2022, **30**, 1435–1449.e9.
37 J. M. C. Kwan, Y. Liang, E. W. L. Ng, E. Sviriaeva, C. Li, Y. Zhao, X.-L. Zhang, X.-W. Liu, S. H. Wong and Y. Qiao, *Chem. Sci.*, 2024, **15**, 1846–1859.
38 A. Bateman, M. J. Martin, S. Orchard, M. Magrane, R. Agivetova, S. Ahmad, E. Alpi, E. H. Bowler-Barnett, R. Britto, B. Bursteinas, H. Bye-A-Jee, R. Coetzee, A. Cukura, A. da Silva, P. Denny, T. Dogan, T. G. Ebenezer, J. Fan, L. G. Castro, P. Garmiri, G. Georghiou, L. Gonzales, E. Hatton-Ellis, A. Hussein, A. Ignatchenko, G. Insana, R. Ishtiaq, P. Jokinen, V. Joshi, D. Jyothi, A. Lock, R. Lopez, A. Luciani, J. Luo, Y. Lussi, A. MacDougall, F. Madeira, M. Mahmoudy, M. Menchi, A. Mishra, K. Moulang, A. Nightingale, C. S. Oliveira, S. Pundir, G. Qi, S. Raj, D. Rice, M. R. Lopez, R. Saidi, J. Sampson, T. Sawford, E. Speretta, E. Turner, N. Tyagi, P. Vasudev, V. Volynkin, K. Warner, X. Watkins, R. Zaru, H. Zellner, A. Bridge, S. Poux, N. Redaschi, L. Aimo, G. Argoud-Puy, A. Auchincloss, K. Axelsen, P. Bansal, D. Baratin, M. C. Blatter, J. Bolleman, E. Boutet, L. Breuza, C. Casals-Casas, E. de Castro, K. C. Echioukh, E. Coudert, B. Cuche, M. Doche, D. Dornevil, A. Estreicher, M. L. Famiglietti, M. Feuermann, E. Gasteiger, S. Gehant, V. Gerritsen, A. Gos, N. Gruaz-Gumowski, U. Hinz, C. Hulo, N. Hyka-Nouspikel, F. Jungo, G. Keller, A. Kerhornou, V. Lara, P. Le Mercier, D. Lieberherr, T. Lombardot, X. Martin, P. Masson, A. Morgat, T. B. Neto, S. Paesano, I. Pedruzzi, S. Pilbout, L. Pourcel, M. Pozzato, M. Pruess, C. Rivoire, C. Sigrist, K. Sonesson, A. Stutz, S. Sundaram, M. Tognolli, L. Verbregue, C. H. Wu, C. N. Arighi, L. Arminski, C. Chen, Y. Chen, J. S. Garavelli, H. Huang, K. Laiho, P. McGarvey, D. A. Natale, K. Ross, C. R. Vinayaka, Q. Wang, Y. Wang, L. S. Yeh and J. Zhang, *Nucleic Acids Res.*, 2021, **49**, D480–D489.
39 T. Uehara and J. T. Park, *J. Bacteriol.*, 2003, **185**, 679–682.

40 C. T. Tan, X. Xu, Y. Qiao and Y. Wang, *Nat. Commun.*, 2021, **12**, 2560.
41 J. Jumper, R. Evans, A. Pritzel, T. Green, M. Figurnov, O. Ronneberger, K. Tunyasuvunakool, R. Bates, A. Žídek, A. Potapenko, A. Bridgland, C. Meyer, S. A. A. Kohl, A. J. Ballard, A. Cowie, B. Romera-Paredes, S. Nikolov, R. Jain, J. Adler, T. Back, S. Petersen, D. Reiman, E. Clancy, M. Zielinski, M. Steinegger, M. Pacholska, T. Berghammer, S. Bodenstein, D. Silver, O. Vinyals, A. W. Senior, K. Kavukcuoglu, P. Kohli and D. Hassabis, *Nature*, 2021, **596**, 583–589.
42 M. Holcomb, Y. Chang, D. S. Goodsell and S. Forli, *Protein Sci.*, 2023, **32**, e4530.
43 O. Trott and A. J. Olson, *J. Comput. Chem.*, 2010, **31**, 455–461.
44 Q. Xu, P. Abdubek, T. Astakhova, H. L. Axelrod, C. Bakolitsa, X. Cai, D. Carlton, C. Chen, H.-J. Chiu, M. Chiu, T. Clayton, D. Das, M. C. Deller, L. Duan, K. Ellrott, C. L. Farr, J. Feuerhelm, J. C. Grant, A. Grzechnik, G. W. Han, L. Jaroszewski, K. K. Jin, H. E. Klock, M. W. Knuth, P. Kozbial, S. S. Krishna, A. Kumar, W. W. Lam, D. Marciano, M. D. Miller, A. T. Morse, E. Nigoghossian, A. Nopakun, L. Okach, C. Puckett, R. Reyes, H. J. Tien, C. B. Trame, H. van den Bedem, D. Weekes, T. Wooten, A. Yeh, K. O. Hodgson, J. Wooley, M.-A. Elsliger, A. M. Deacon, A. Godzik, S. A. Lesley and I. A. Wilson, *Acta Cryst. F*, 2010, **66**, 1354–1364.
45 R. A. Laskowski and M. B. Swindells, *J. Chem. Inf. Model.*, 2011, **51**, 2778–2786.
46 F. Bottacini, M. Ventura, D. van Sinderen and M. O'Connell Motherway, *Microb. Cell Fact.*, 2014, **13**, S4.
47 S. Klupt, K. T. Fam, X. Zhang, P. K. Chodisetti, A. Mehmood, T. Boyd, D. Grotjahn, D. Park and H. C. Hang, *eLife*, 2024, **13**, RP95297.